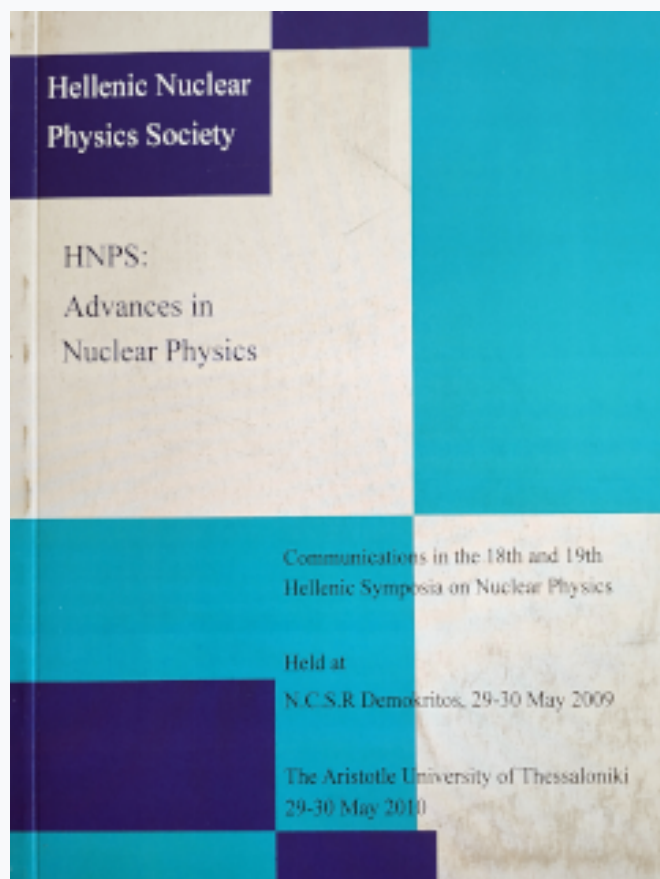


## HNPS Advances in Nuclear Physics

Vol 17 (2009)

HNPS2009



### To cite this article:

Bonatsos, D., Boztosun, I., & Inci, I. (2019). A long sought result: Closed analytical solutions of the Bohr Hamiltonian with the Morse potential. *HNPS Advances in Nuclear Physics*, 17, 15-20. <https://doi.org/10.12681/hnps.2566>

# A long sought result: Closed analytical solutions of the Bohr Hamiltonian with the Morse potential

**Dennis Bonatsos<sup>a</sup>, I. Boztosun<sup>b</sup>, I. Inci<sup>b</sup>**

<sup>a</sup>*Institute of Nuclear Physics, N.C.S.R. “Demokritos”, GR-15310 Aghia Paraskevi, Attiki, Greece*

<sup>b</sup>*Department of Physics, Erciyes University, Kayseri, Turkey*

---

## Abstract

Closed analytical solutions of the Morse potential for nonzero angular momenta has been an open problem for decades, solved recently by the Asymptotic Iteration Method (AIM) for solving differential equations. Closed analytical expressions have been obtained for the energy eigenvalues and B(E2) rates of the Bohr Hamiltonian in the  $\gamma$ -unstable case, as well as in an exactly separable rotational case with  $\gamma \approx 0$ , called the exactly separable Morse (ES-M) solution. All medium mass and heavy nuclei with known  $\beta_1$  and  $\gamma_1$  bandheads have been fitted by using the two-parameter  $\gamma$ -unstable solution for transitional nuclei and the three-parameter ES-M for rotational ones. It is shown that bandheads and energy spacings within the bands are well reproduced for more than 50 nuclei in each case. Comparisons to the fits provided by the Davidson and Kratzer potentials, also soluble by the AIM, are made.

---

The recent introduction of the critical point symmetries E(5) [1] and X(5) [2], which describe shape phase transitions between vibrational and  $\gamma$ -unstable/prolate deformed rotational nuclei respectively, has stirred much interest in special solutions of the Bohr Hamiltonian, describing collective nuclear properties in terms of the collective variables  $\beta$  and  $\gamma$ . Such solutions can describe nuclei in the whole region between different limiting symmetries, while critical point symmetries are appropriate for describing nuclei only at or near the critical point, in good agreement with experiment [3].

It has been known for a long time [4] that simple special solutions of the Bohr Hamiltonian, resulting from exact separation of variables in the relevant Schrödinger equation, can be obtained in the  $\gamma$ -unstable case, in which the potential depends only on  $\beta$ , as well as in the case in which the potential can be written in the separable form  $u(\beta, \gamma) = u(\beta) + u(\gamma)/\beta^2$ , in the special cases of  $\gamma \approx 0$  or  $\gamma \approx \pi/6$  [5]. An approximate separation of variables has also been attempted for potentials of the form  $u(\beta, \gamma) = u(\beta) + u(\gamma)$  in the cases of  $\gamma \approx 0$  [2] or  $\gamma \approx \pi/6$  [6]. Sev-

The potentials mentioned above are known to be exactly soluble for all values of angular momentum  $L$ . In the present work, we introduce special solutions for the Morse potential,  $u(\beta) = e^{-2a(\beta-\beta_e)} - 2e^{-a(\beta-\beta_e)}$ , which is known [9, 10] to be exactly soluble only for  $L = 0$ . The overall factor  $D$  of the Morse potential is set equal to unity, without affecting the method of solution, since it can be scaled out if ratios of energies are used, as in the present work. Analytical expressions for the spectra for any  $L$  are obtained by solving the relevant differential equation through the Asymptotic Iteration Method (AIM) [11, 12], after applying the Pekeris approximation [13]. Solutions for the  $\gamma$ -unstable case and the exactly separable case with  $\gamma \approx 0$  (to be called ES-M) have been obtained [14].

A few advantages of the present approach are listed here.

1) A well known problem of X(5) and related solutions is the overprediction of the energy spacings within the beta band by almost a factor of two [3]. It is known that this problem can be avoided by replacing the infinite-well potential of X(5) by a potential with sloped walls [15]. The present solution avoids this problem, since the right branch of the Morse potential imitates the sloped wall.

2) In X(5) and related models, using potentials of the form  $u(\beta, \gamma) = u(\beta) + u(\gamma)$ , the ground state and beta bands depend only on the parameters of the  $\beta$  potential, while the gamma bands depend also on an additional parameter introduced by the  $\gamma$  potential [usually the stiffness of the harmonic oscillator used as  $u(\gamma)$ ]. When exactly separable potentials of the form  $u(\beta, \gamma) = u(\beta) + u(\gamma)/\beta^2$  are used, all bands (ground state, beta, gamma) depend on all parameters. Thus, all bands are treated on an equal footing, as in the case of the ES-D solution [16].

The original collective Bohr Hamiltonian is

$$H = -\frac{\hbar^2}{2B} \left[ \frac{1}{\beta^4} \frac{\partial}{\partial \beta} \beta^4 \frac{\partial}{\partial \beta} + \frac{1}{\beta^2 \sin 3\gamma} \frac{\partial}{\partial \gamma} \sin 3\gamma \frac{\partial}{\partial \gamma} \right. \\ \left. - \frac{1}{4\beta^2} \sum_{k=1,2,3} \frac{Q_k^2}{\sin^2 \left( \gamma - \frac{2}{3}\pi k \right)} \right] + V(\beta, \gamma), \quad (1)$$

where  $\beta$  and  $\gamma$  are the usual collective coordinates which define the shape of the nuclear surface.  $Q_k$  ( $k=1, 2, 3$ ) represents the angular momentum components in the intrinsic frame, and  $B$  is the mass parameter. Reduced energies and reduced potentials are defined as  $\epsilon = 2BE/\hbar^2$ ,  $v = 2BV/\hbar^2$  respectively [1].

We first examine the  $\gamma \approx 0$  case. In the case of the exactly separable potentials  $u(\beta, \gamma) = u(\beta) + u(\gamma)/\beta^2$  mentioned above, the wave functions take the form

$\psi(\beta, \gamma, \theta_j) = \xi_L(\beta)\Gamma_K(\gamma)D_{M,K}^L(\theta_j)$ , where  $\theta_j$  ( $j = 1, 2, 3$ ) are the Euler angles,  $D(\theta_j)$  represents Wigner functions of these angles,  $L$  stands for the eigenvalues of the angular momentum, while  $M$  and  $K$  are the eigenvalues of the projections of the angular momentum on the laboratory-fixed  $z$ -axis and the body-fixed  $z'$ -axis respectively. The Schrödinger equation is thus separated, as in Refs. [4, 7], into a “radial” part (depending on  $\beta$ ) and a  $\gamma$  part.

17

In the case of the Morse potential, using the Pekeris approximation [13] and solving the  $\beta$  equation through AIM (the details are given in Ref. [14]), we obtain the energy eigenvalues

$$\epsilon_{n,L} = \frac{\mu c_0}{\beta_e^2} - \left[ \frac{\gamma_1^2}{2\beta_e \gamma_2} - \left( n + \frac{1}{2} \right) \frac{\alpha}{\beta_e} \right]^2, \quad (2)$$

where

$$c_0 = 1 - \frac{3}{\alpha} + \frac{3}{\alpha^2}, \quad c_1 = \frac{4}{\alpha} - \frac{6}{\alpha^2}, \quad c_2 = -\frac{1}{\alpha} + \frac{3}{\alpha^2}, \quad \alpha = a\beta_e, \quad (3)$$

$$\gamma_1^2 = 2\beta_e^2 - \mu c_1, \quad \gamma_2^2 = \beta_e^2 + \mu c_2, \quad \mu = \frac{L(L+1)}{3} + 2 + \lambda. \quad (4)$$

$\lambda$  in the last equation comes from the exact separation of variables and is determined from the  $\gamma$  equation. We use the same  $\gamma$  potential  $u(\gamma) = (3c)^2\gamma^2$  as in the Davidson case [16], leading to

$$\lambda = \epsilon_\gamma - \frac{K^2}{3}, \quad \epsilon_\gamma = (3C)(n_\gamma + 1), \quad C = 2c. \quad (5)$$

We now turn our attention to  $\gamma$ -unstable solutions. In this case, the reduced potential is assumed to be  $\gamma$  independent,  $v(\beta, \gamma) = u(\beta)$ . Then the wavefunction takes the form [4]  $\psi(\beta, \gamma, \theta_j) = R(\beta)\Phi(\gamma, \theta_j)$ . The equation which includes the Euler angles and  $\gamma$  has been solved by Bès [17]. In this equation, the eigenvalues of the second-order Casimir operator of  $SO(5)$  occur, having the form  $\Lambda = \tau(\tau + 3)$ , where  $\tau$  is the seniority quantum number, characterizing the irreducible representations of  $SO(5)$  and taking the values  $\tau = 0, 1, 2, 3, \dots$  [18].

The values of the angular momentum  $L$  are given by the algorithm

$$\tau = 3\nu_\Delta + \lambda, \quad \nu_\Delta = 0, 1, 2, \dots \quad L = \lambda, \lambda + 1, \dots, 2\lambda - 2, 2\lambda \quad (6)$$

(with  $2\lambda - 1$  missing), where  $\nu_\Delta$  is the missing quantum number in the reduction  $SO(5) \supset SO(3)$  [18]. The ground state band levels are determined by  $L = 2\tau$  and  $n = 0$ .

Using the Pekeris approximation [13] and AIM (see Ref. [14] for the details), we

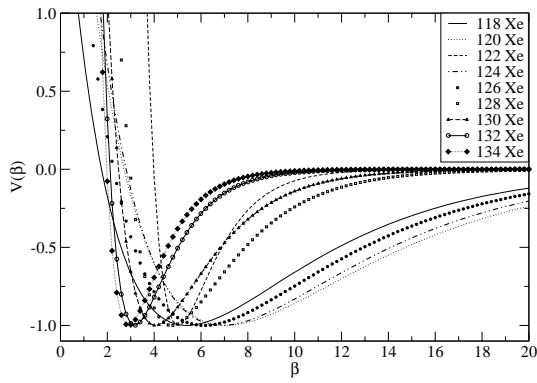


Fig. 1. Evolution of Morse potential shapes for the  $^{54}\text{Xe}$  isotopes, with the parameters given in Ref. [14].

obtain the energy eigenvalues

$$\epsilon_{n,\tau} = \frac{\nu c_0}{\beta_e^2} - \left[ \frac{\gamma_1^2}{2\beta_e \gamma_2} - \left( n + \frac{1}{2} \right) \frac{\alpha}{\beta_e} \right]^2, \quad (7)$$

where

$$\gamma_1^2 = 2\beta_e^2 - \nu c_1, \quad \gamma_2^2 = \beta_e^2 + \nu c_2, \quad \nu = \tau(\tau + 3) + 2, \quad (8)$$

with the rest of the quantities given again by Eq. (3).

In order to test the applicability of the Morse potential in the description of nuclear spectra, we have fitted all nuclei with mass  $A \geq 100$  and  $R_{4/2} = E(4)/E(2) < 2.6$ , for which at least the  $\beta_1$  and  $\gamma_1$  bandheads are known, using the  $\gamma$ -unstable solution of the Morse potential, which involves two free parameters ( $\beta_e, a$ ). Results for 54 nuclei are shown in Ref. [14].

The Morse potentials obtained for the  $^{54}\text{Xe}$  isotopes are shown in Fig. 1. The evolution of the parameters and the shapes of the potentials are clear. As one moves from  $^{134}\text{Xe}_{80}$ , which is just below the  $N = 82$  magic number, to the mid-shell nucleus  $^{120}\text{Xe}_{66}$ , the  $\beta_e$  parameter (which is the position of the minimum of the potential) increases, while the parameter  $a$ , which corresponds to the steepness of the potential, decreases. As a result, one gradually obtains less steep potentials with a minimum further away from the origin. The trends start to be reversed at  $^{118}\text{Xe}_{64}$ , which is just below mid-shell.

We have also fitted all nuclei with mass  $A \geq 150$  and  $R_{4/2} = E(4)/E(2) > 2.9$  for which at least the  $\beta_1$  and  $\gamma_1$  bandheads are known, using the exactly separable rotational solution of the Morse potential with  $\gamma \approx 0$  (ES-M), which involves three free parameters (the Morse parameters  $\beta_e$  and  $a$ , as well as the stiffness  $C$  of the  $\gamma$  potential). All bands are treated on an equal footing, depending on all three parameters. Results for 45 rare earths and 13 actinides are shown in Ref. [14].

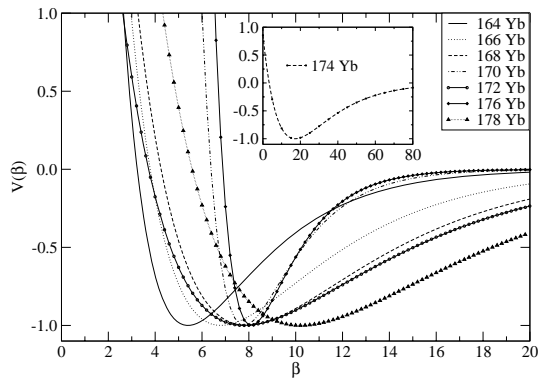


Fig. 2. Evolution of Morse potential shapes for the  $^{70}\text{Yb}$  isotopes, with the parameters given in Ref. [14].

The Morse potentials obtained for the  $^{70}\text{Yb}$  isotopes are shown in Fig. 2. The evolution of the parameters and the shapes of the potentials are again clear. As one moves from  $^{164}\text{Yb}_{94}$  to the mid-shell nucleus  $^{174}\text{Yb}_{104}$ , the  $\beta_e$  parameter (which is the position of the minimum of the  $\beta$ -potential) again increases, while the parameter  $a$ , which corresponds to the steepness of the  $\beta$ -potential, again decreases. The  $C$  parameter, which is related to the stiffness of the  $\gamma$ -potential, increases. As a result, one gradually obtains less steep  $\beta$ -potentials with a minimum further away from the origin, while the  $\gamma$ -potentials get stiffer at the same time.

A notable exception occurs in the  $N = 90$  isotones  $^{150}\text{Nd}$ ,  $^{152}\text{Sm}$ ,  $^{154}\text{Gd}$ , which are known to be good examples of the X(5) critical point symmetry, along with  $^{178}\text{Os}$  [3]. The relative failure of the Morse potential to describe critical nuclei is expected. The potential at the critical point is expected to be flat, as the infinite-well potential used in X(5), or to have a little bump in the middle [3]. Microscopic relativistic mean field calculations [19] of potential energy surfaces support these assumptions. Since the Morse potential cannot imitate a flat potential, with or without a bump in the middle, it is expected that it cannot describe these nuclei satisfactorily.

A comparison of the present fits (reported in Ref. [14]) to the results provided by the Davidson potential in the exactly separable  $\gamma \approx 0$  case [16] (ES-D), which contains two free parameters ( $\beta_0$ ,  $c$ ) instead of three (see Table 1 of Ref. [16]), shows that the extra parameter extends the region of applicability of the model in most nuclei to higher angular momenta, largely improving the quality of the fits.

In summary, the Bohr Hamiltonian has been solved with the Morse potential for any angular momentum, both in the  $\gamma$ -unstable case and in the exactly separable rotational case with  $\gamma \approx 0$  (in which a harmonic oscillator is used for the  $\gamma$  potential), labelled as ES-M. The solution has been achieved [14] through the Asymptotic Iteration Method (AIM) and has involved the Pekeris approximation.

Numerical results have been presented for both solutions, including all relevant

medium mass and heavy nuclei for which at least the  $\beta_1$  and  $\gamma_1$  bandheads are known. The success of the present solutions in reproducing quite well both the bandheads of and the spacings within the ground,  $\beta_1$  and  $\gamma_1$  bands indicate that a detailed study of  $\gamma_2$  and other higher bands within this framework might be fruitful. The influence of the finite depth of the potential is also worth considering in further detail. From the findings of Ref. [20], where the E(5) case was solved for a finite well, the influence of the finite depth of the potential is expected to show up more clearly in the higher excited states. Work on the calculation of wave functions and  $B(E2)$  transition rates is in progress.

20

## References

- [1] F. Iachello, Phys. Rev. Lett. **85**, 3580 (2000).
- [2] F. Iachello, Phys. Rev. Lett. **87**, 052502 (2001).
- [3] R. F. Casten and E. A. McCutchan, J. Phys. G: Nucl. Part. Phys. **34**, R285 (2007).
- [4] L. Wilets and M. Jean, Phys. Rev. **102**, 788 (1956).
- [5] J. Meyer-ter-Vehn, Nucl. Phys. **A 249**, 111 (1975).
- [6] D. Bonatsos, D. Lenis, D. Petrellis, and P. A. Terziev, Phys. Lett. **B 588**, 172 (2004).
- [7] L. Fortunato, Eur. Phys. J. A **26**, s01, 1 (2005).
- [8] D. Bonatsos, D. Lenis, and D. Petrellis, Romanian Reports in Physics **59**, 273 (2007). ArVix nucl-th/0701055.
- [9] S. Flügge, *Practical Quantum Mechanics* (Springer, Berlin, 1974).
- [10] F. Cooper, A. Khare, and U. Sukhatme, *Supersymmetry in Quantum Mechanics* (World Scientific, Singapore, 2001).
- [11] H. Ciftci, R. L. Hall and N. Saad, J. Phys. A: Math. Gen. **36**, 11807 (2003).
- [12] H. Ciftci, R. L. Hall and N. Saad, J. Phys. A: Math. Gen. **38**, 1147 (2005).
- [13] C. L. Pekeris, Phys. Rev. **45**, 98 (1934).
- [14] I. Boztosun, D. Bonatsos, and I. Inci, Phys. Rev. C **77**, 044302 (2008).
- [15] M. A. Caprio, Phys. Rev. C **69**, 044307 (2004).
- [16] D. Bonatsos, E. A. McCutchan, N. Minkov, R. F. Casten, P. Yotov, D. Lenis, D. Petrellis, and I. Yigitoglu, Phys. Rev. C **76**, 064312 (2007).
- [17] D. R. Bès, Nucl. Phys. **10**, 373 (1959).
- [18] G. Rakavy, Nucl. Phys. **4**, 289 (1957).
- [19] R. Fossion, D. Bonatsos, and G. A. Lalazissis, Phys. Rev. C **73**, 044310 (2006).
- [20] M. A. Caprio, Phys. Rev. C **65**, 031304 (2002).